

The spin-down accretion regime of Galactic ultra-luminous X-ray pulsar Swift J0243.6+6124

JIREN LIU,¹ LONG JI,² AND MINGYU GE³

¹*Beijing Planetarium, Beijing Academy of Science and Technology, Beijing 100044, China*

²*School of Physics and Astronomy, Sun Yat-sen University, 2 Daxue Road, Zhuhai, Guangdong 519082, China*

³*Institute of High Energy Physics, Chinese Academy of Sciences, Beijing 100049, China*

ABSTRACT

The relative high fluxes of the Galactic ultra-luminous X-ray pulsar Swift J0243 allow a detailed study of its spin-down regime in quiescence state, for a first time. After the 2017 giant outburst, its spin frequencies show a linear decreasing trend with some variations due to minor outbursts. The linear spin-down rate is $\sim -1.9 \times 10^{-12}$ Hz/s during the period of lowest luminosity, from which one can infer a dipole field $\sim 1.75 \times 10^{13}$ G. The $\dot{\nu} - L$ relation during the spin-down regime is complex, and the $\dot{\nu}$ is close to 0 when the luminosity reaches both the high end ($L_{38} \sim 0.3$) and the lowest value ($L_{38} \sim 0.03$). The luminosity of zero-torque is different for the giant outburst and other minor outbursts. It is likely due to different accretion flows for different types of outburst, as evidenced by the differences of the spectra and pulse profiles at a similar luminosity for different types of outburst (giant or not). The pulse profile changes from double peaks in the spin-up state to a single broad peak in the low spin-down regime, indicating the emission beam/region is larger in the low spin-down regime. These results show that accretion is still ongoing in the low spin-down regime for which the neutron star is supposed to be in a propeller state.

Keywords: Accretion – pulsars: individual: Swift J0243+6124 – X-rays: binaries

1. INTRODUCTION

Accretion-powered X-ray pulsars are strongly magnetized neutron stars that accrete material from normal companion stars. The accreting material also contains angular momentum that changing the spin period of the neutron star. The spin-up/spin-down behavior of the neutron star depends on the interaction between the accreting flow and the magnetosphere of the neutron star (e.g. Rappaport & Joss 1977; Ghosh & Lamb 1979; Wang et al. 1995). Therefore, the observed spin behavior can be used to constrain the interaction of the accreting flow with the magnetosphere of X-ray pulsars.

Be-type X-ray binaries (BeXBs) are ideal targets for the study of the spin behavior of X-ray pulsars since they cover a large dynamical range of luminosity (accretion rate). In BeXBs, the Be/Oe-type donor star rotates rapidly and forms an equatorial accretion disk, and the neutron star, generally in an eccentric orbit, will pro-

duce a normal outburst (type I, with peak luminosities below 10^{37} erg s⁻¹) around the periastron passage. Occasionally, they can produce a giant outburst (type II), which could occur at any orbital phase and reach a peak luminosity higher than 10^{38} erg s⁻¹ (e.g. Reig & Nespoli 2011). During the outbursts, the pulsars generally undergo spin-up episodes, the rates of which correlate with luminosity (e.g. Bildsten et al. 1997). In-between the outbursts, the pulsars are generally in a quiescence state and a spin-down trend is observed.

Due to the relatively low luminosity, the spin-down accretion regime of BeXBs is difficult to monitor and is rarely explored compared with the spin-up regime. The spin-down accretion regime, however, is critical to reveal the interaction of the accreting flow with the magnetosphere around the co-rotation radius, beyond which the threading of the disk by the magnetic field applies a negative torque to the neutron star. In this paper, we study the spin-down regime of the Galactic ultra-luminous X-ray pulsar Swift J0243.6+6124 (hereafter J0243), the quiescence state of which is bright enough to provide a unique opportunity to study the spin-down accretion regime, for a first time.

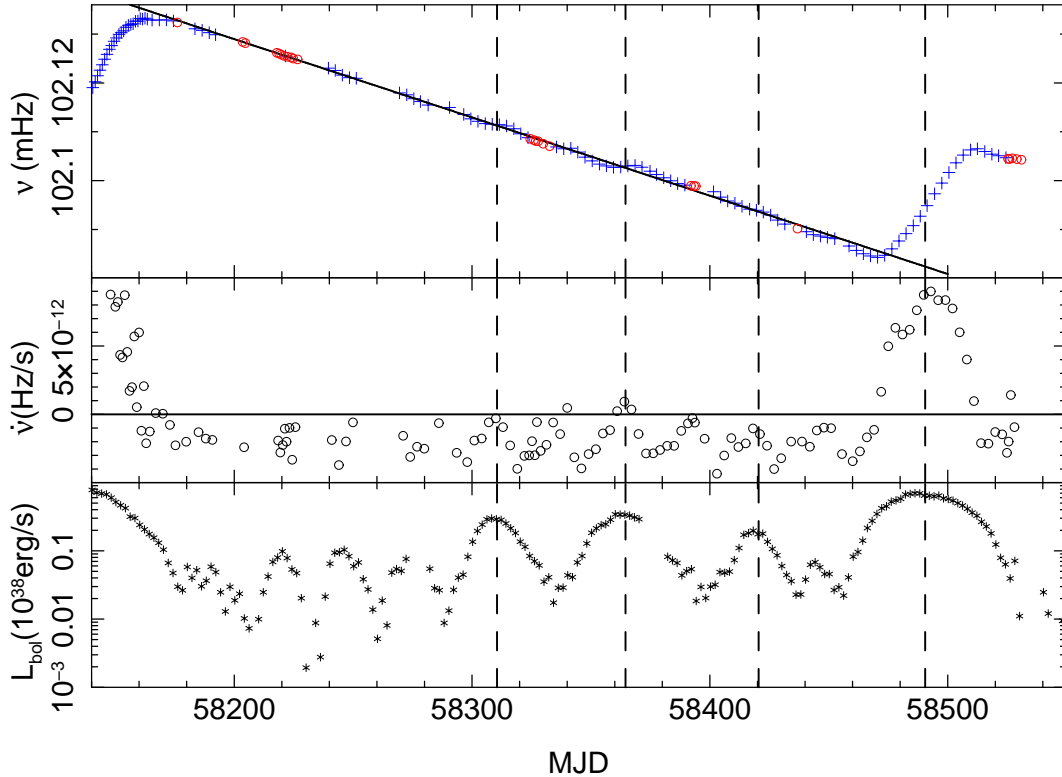


Figure 1. The spin frequency, spin derivative, and bolometric luminosity of Swift J0243 during the giant outburst in 2017. A 300-days long spin-down period is present after the giant outburst, with a last outburst near MJD 58500. The red circles in the top panel are measurements from *Nicer* data. The four vertical dashed lines (around MJD 58310, 58365, 58420, 58490) indicate the four later outbursts.

Swift J0243 is a new BeXB discovered by Swift in October 2017 during one of the brightest outburst (Cenko et al. 2017). At a distance of 5.2 kpc (Bailer-Jones et al. 2021), its peak luminosity reaches $\sim 10^{39} \text{ergs}^{-1}$, which makes it the first Galactic ultra-luminous X-ray pulsar (e.g. Tsygankov et al. 2018; Wilson-Hodge et al. 2018). We note that a larger distance of 6.8 kpc were generally adopted in earlier studies as measured from *Gaia* data release 2 (Bailer-Jones et al. 2018). After the giant outburst, it underwent several minor outbursts and one last relatively bright outburst around Jan. 2019. Between the giant outburst and the last brighting, a long spin-down trend was observed (Figure 1).

2. OBSERVATION DATA

The 2017 giant outburst of Swift J0243 has been monitored by many existing X-ray instruments, including *Fermi*, *Swift*, *Nicer*, *MAXI*, and *Insight-HXMT*. The Gamma-ray Burst Monitor (GBM, Meegan et al. 2009) on-board the *Fermi* spacecraft provides a continuous

monitoring of the spin history of X-ray pulsars¹ (e.g. Finger et al. 2009; Malacaria et al. 2020). The spin evolution of J0243 measured by GBM is presented in Figure 1, together with the bolometric luminosity converted from the *Swift*/BAT flux in 15-50 keV (see next section). For completeness, we added a few measurements from *Nicer* data (red circles in Figure 1) when the spin frequency was not detected by *Fermi*/GBM. The spin derivatives, calculated from two contiguous measurements, are plotted in the middle panel. As can be seen, most of the spin derivatives were negative after the giant outburst (later than MJD 58160), except for the last brighting around MJD 58500.

To convert the BAT flux to bolometric luminosity, we compare the 0.5-150 keV luminosities measured by HXMT with the BAT fluxes at the corresponding HXMT observation time. The luminosities of HXMT observation were taken from Liu et al. (2022). As shown in Figure 2, below $2 \times 10^{38} \text{ergs}^{-1}$, the BAT fluxes and HXMT luminosities follow a relation of $L_{38} = 4.3 \times$

¹ <https://gammaray.msfc.nasa.gov/gbm/science/pulsars/>

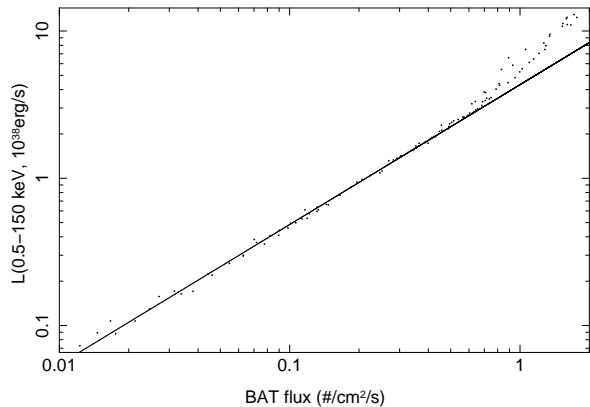


Figure 2. Comparison of the HXMT-estimated bolometric luminosities of Swift J0243 with the BAT fluxes.

$f_{BAT}^{0.95}$, where L_{38} is the bolometric luminosity in units of 10^{38}erg s^{-1} . So we convert the BAT flux to bolometric luminosity with this relation.

3. RESULTS

3.1. Spin-down behavior

As can be seen from Figure 1, after the giant outburst, the spin frequencies show a linear decreasing trend, with some variations due to the middle minor outbursts. We fit a linear function to the data points within MJD 58190 and 58290, where the fluxes are relatively low (the averaged luminosity is about $3 \times 10^{36}\text{ erg s}^{-1}$). We obtain a spin-down rate of $-1.9 \times 10^{-12}\text{ Hz/s}$, which is plotted as the solid line in the top panel of Figure 1.

Besides the linear decreasing trend, we observe two kinds of fluctuations of the spin-down rates. One is around the peak of the minor outbursts, where the spin-down rates increased, or even reversed to spin-up, due to the increasing accretion rate, as indicated by the vertical dashed lines in Figure 1. We see another kind of fluctuation from the middle panel of Figure 1. Between the flux outbursts, around the flux minima (such as around MJD 58335 and 58390), the spin derivatives are also reaching 0, similar to those around outburst peaks. Such a behavior is unexpected.

3.2. Spin-down derivative vs luminosity

To quantify the relation between the spin-down derivative and accretion luminosity, we plot the $\dot{\nu} - L$ relation during different spin-down periods in Figure 3. The spin derivative $\dot{\nu}$ is calculated from two contiguous measurements, the time interval between which is smaller than 10 days. The luminosity is calculated as an averaged value over the period. To check the differences of different outbursts and luminosities, we divided the time range into MJD 58150-58170 (the fading

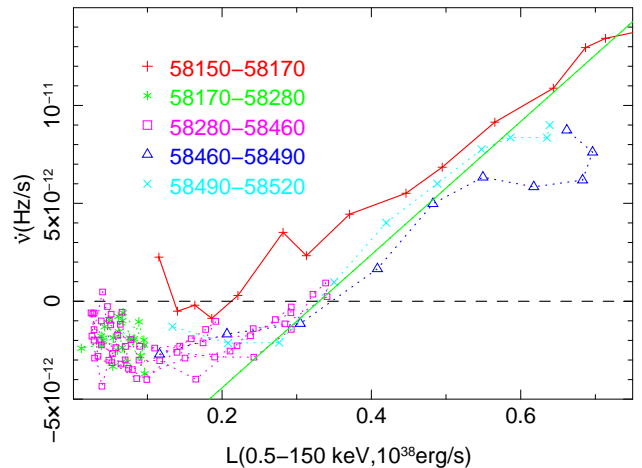


Figure 3. The $\dot{\nu} - L$ relation of Swift J0243 observed during different spin-up/spin-down periods. A solid green line is drawn to help to guide eyes.

period of the giant outburst), 58170-58280 (the relatively low luminosity period), 58280-58460 (the middle minor outbursts), 58460-58490 (the growing period of the last outburst) and 58490-58520 (the fading period of the last outburst). For the period between MJD 58150 and 58170, the calculated $\dot{\nu}$ from GBM data show larger fluctuations and we used the $\dot{\nu}$ calculated from HXMT data.

First, we see that the $\dot{\nu} - L$ relation of the giant outburst shows an offset from that of the last outburst around MJD 58500. The zero point of $\dot{\nu} = 0$ is around a luminosity $\sim 0.2 \times 10^{38}\text{ erg s}^{-1}$ for the giant outburst, while it is around $0.33 \times 10^{38}\text{ erg s}^{-1}$ for the last outburst and for the minor outburst around MJD 58365.

During the relatively low period between MJD 58170 and 58280, the measured $\dot{\nu}$ are scattered around $-2 \times 10^{-12}\text{ Hz/s}$, with the luminosities below $0.1 \times 10^{38}\text{ erg s}^{-1}$. For the period between MJD 58280 and 58460, above $0.2 \times 10^{38}\text{ erg s}^{-1}$, the spin-down derivative decreases when the luminosity decreases; while below $0.1 \times 10^{38}\text{ erg s}^{-1}$, the averaged trend of spin-down rate seems to increase when the luminosity decreases to the lowest value, as already noted in previous section. And there seems to be two zero points of $\dot{\nu} = 0$: one for $0.33 \times 10^{38}\text{ erg s}^{-1}$ and one for $0.03 - 0.04 \times 10^{38}\text{ erg s}^{-1}$.

For the last outburst between MJD 58460 and 58520, for $\dot{\nu} > 0$, the slope of the $\dot{\nu} - L$ relation is similar to that of the giant outburst; while for $\dot{\nu} < 0$, the slope becomes flattened when the luminosity is below $0.25 \times 10^{38}\text{ erg s}^{-1}$.

3.3. Evolution of the pulse profile

The pulse profiles of J0243 had been extensively studied in previous work, but no attention was paid for

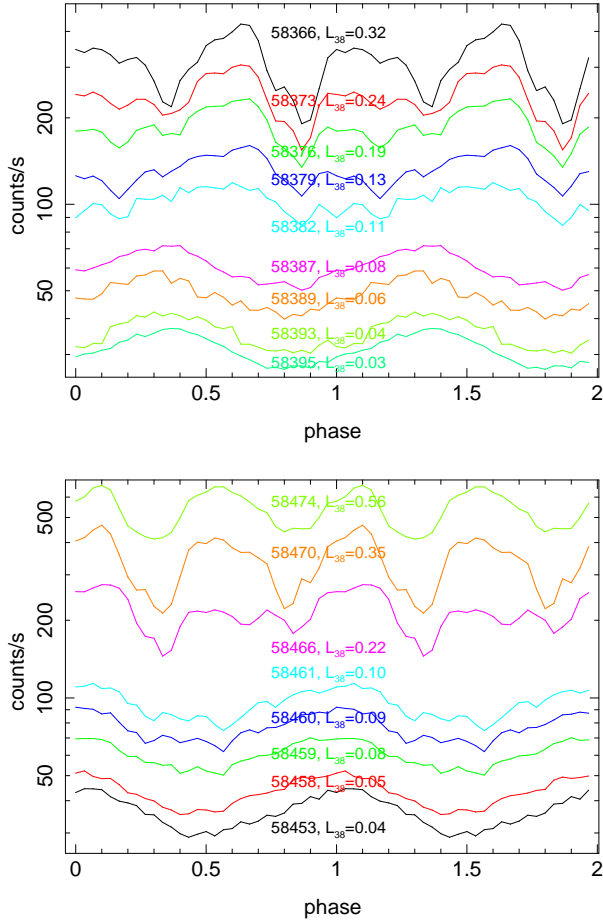


Figure 4. Example of the pulse profile evolution of Swift J0243 during the spin-down/spin-up transition regime within 0.4–8 keV observed by *Nicer*. The chosen periods are around MJD 58366–58395 (top) and MJD 58453–58474 (bottom).

the transition period between spin-up and spin-down regimes. We find that the profile mostly depends on the luminosity, and here we choose two periods (MJD 58366–58395 and 58453–58470) to illustrate the evolution of the profile during the spin-down regime. The profile evolution during other periods are similar. The aligned pulse profiles within 0.4–8 keV observed by *Nicer* are plotted in Figure 4.

During the lowest state of luminosity ($L_{38} \sim 0.03 - 0.08$), the profile is a single broad peak, with a phase width ~ 1 . Around the luminosity of $L_{38} \sim 0.08 - 0.11$, a minor peak appeared left to the main peak. During the middle state of luminosity ($L_{38} \sim 0.2$), the main peak splits into one minor peak and one main peak, and the phase width of the main peak is about 0.5 in this state. And the profile looks composed of three peaks. At the luminosity of $L_{38} \sim 0.32 - 0.35$, when the spin frequency changing from spin-down to spin-up, the newly appeared

Table 1. Fitting parameters of cutoff power-law model

MJD	L_{38}	N_H^a	Norm ^b	Γ	E_c (keV)
58494	0.6	0.62 ± 0.01	0.464 ± 0.004	0.80 ± 0.01	15.5 ± 0.1
58500	0.5	0.59 ± 0.01	0.375 ± 0.003	0.70 ± 0.01	13.8 ± 0.1
58506	0.4	0.64 ± 0.01	0.293 ± 0.003	0.62 ± 0.01	12.5 ± 0.1
58510	0.3	0.62 ± 0.01	0.221 ± 0.003	0.56 ± 0.01	11.5 ± 0.1
58516	0.2	0.78 ± 0.04	0.115 ± 0.004	0.50 ± 0.02	10.5 ± 0.3
58520	0.1	0.75 ± 0.06	0.078 ± 0.004	0.51 ± 0.04	9.9 ± 0.4
58521	0.07	0.72 ± 0.08	0.057 ± 0.004	0.51 ± 0.06	9.4 ± 0.6
58523	0.05	0.83 ± 0.12	0.048 ± 0.005	0.65 ± 0.08	10.8 ± 1.0
58151	0.4	0.43 ± 0.02	0.277 ± 0.005	0.59 ± 0.01	11.7 ± 0.2
58506	0.4	0.64 ± 0.01	0.293 ± 0.003	0.62 ± 0.01	12.5 ± 0.1
58157	0.25	0.45 ± 0.03	0.145 ± 0.005	0.46 ± 0.03	10.8 ± 0.3
58513	0.25	0.67 ± 0.02	0.140 ± 0.002	0.41 ± 0.02	10.1 ± 0.2
58165	0.13	0.51 ± 0.04	0.094 ± 0.004	0.50 ± 0.03	10.2 ± 0.4
58519	0.13	0.74 ± 0.04	0.089 ± 0.003	0.47 ± 0.03	9.6 ± 0.3

: ^a N_H is the hydrogen column density in units of 10^{22} cm^{-2} ;

: ^b Norm is the normalization of the power-law model at 1 keV, in units of photons $\text{keV}^{-1} \text{ cm}^{-2} \text{ s}^{-1}$.

two minor peaks merged into one bump, and the profile is composed of double peaks. At higher luminosity of $L_{38} \sim 0.56$, the profile is double-peaked, similar to that around $L_{38} \sim 0.32 - 0.35$.

That is, the profile of Swift J0243 changes from a single broad peak to double peaks when it changes from the lowest luminosity state of spin-down to the spin-up state, and in-between, the profile shows a transitional shape. It indicates the change of accretion geometry/emission region during the spin-down/spin-up transition.

3.4. Evolution of the spectrum

To study the spectral evolution of Swift J0243 during the spin-down regime, we use the HXMT observation of the last outburst, which covered MJD 58493 to 58523. These observations are almost on a daily base and have a wide energy coverage. HXMT has three collimated instruments sensitive to different energy bands: LE (1–10 keV), ME (10–30 keV), and HE (25–250 keV), with effective areas of 384, 952, and 5100 cm^2 , respectively (Zhang et al. 2020). The spectra are extracted using the HXMT Data Analysis software v2.04, with the calibration model of v2.05 and only use the data from LE and ME. The spectra are binned with a minimum signal-to-noise of 10. Some examples of the spectra at different times and luminosities are presented in Figure 5. All the spectra can be well fitted with an absorbed cutoff-power-law model, with a reduced χ^2 smaller than 1.2. The fitting results are listed in Table 1.

As can be seen from Table 1, for the spectrum at $L_{38} = 0.6$ to that at $L_{38} = 0.07$, the fitted absorption column changes from $0.6 \times 10^{22} \text{ cm}^{-2}$ to $0.72 \times 10^{22} \text{ cm}^{-2}$,

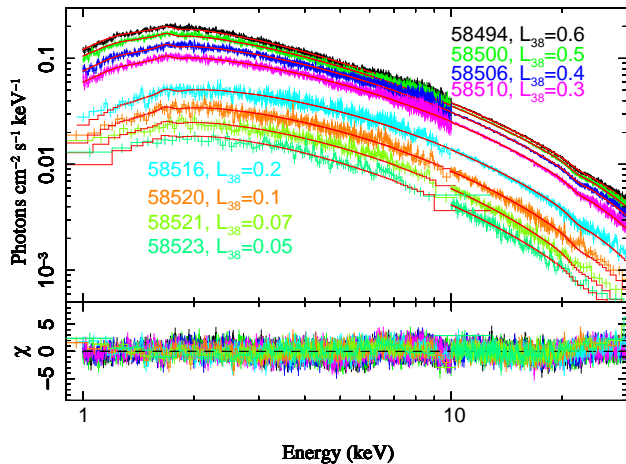


Figure 5. Example of the spectral evolution of Swift J0243 during the spin-up/spin-down transition at different times/luminosities.

the fitted photon index changes from 0.8 to 0.5, and the cutoff energy changes from 15.5 keV to 9.4 keV. The changing trend of the photon index and the cutoff energy is continuous, except for those value at the lowest luminosity of $L_{38} = 0.05$. The lower the luminosity, the harder the spectra, and the smaller the cutoff energy.

4. DISCUSSION AND CONCLUSION

We performed a detailed study of the spin-down accretion regime of Swift J0243 after its giant outburst. The great brightness of Swift J0243 makes its quiescence period observable and thus allows measurement of its spin frequency during the quiescent spin-down regime.

Its spin frequencies after the giant outburst (after MJD 58170) show a linear decreasing trend, superposed with some variations due to the minor outbursts. The linear spin-down rate during the period of lowest luminosity (MJD 58190-58290) is about -1.9×10^{-12} Hz/s. This spin-down rate is likely dominated by the braking torque due to the field threading of the accretion disk outside the co-rotation radius. As the dipole field decreases as r^{-3} , the braking torque is mainly dominated by the threading near the co-rotation radius (R_c). Taking the braking torque as $\tau_b = -\mu^2/9R_c^3$ (Wang et al. 1995; Rappaport et al. 2004) and an accretion torque of $\dot{m}\sqrt{GMR_c}$ (assuming there exist accretion disk terminating at R_c), one can infer a dipole magnetic field of $B \sim 1.75 \times 10^{13}$ G from $2\pi I\dot{\nu} = \dot{m}\sqrt{GMR_c} + \tau_b$, assuming a neutron star of $1.4 M_\odot$ with a radius of 10 km. Such a dipole field is similar to the value inferred from the spin-up torque at higher luminosity with a radiation-pressure-dominated (RPD) disk model (Liu et al. 2022), and is consistent with the cyclotron line of Swift J0243

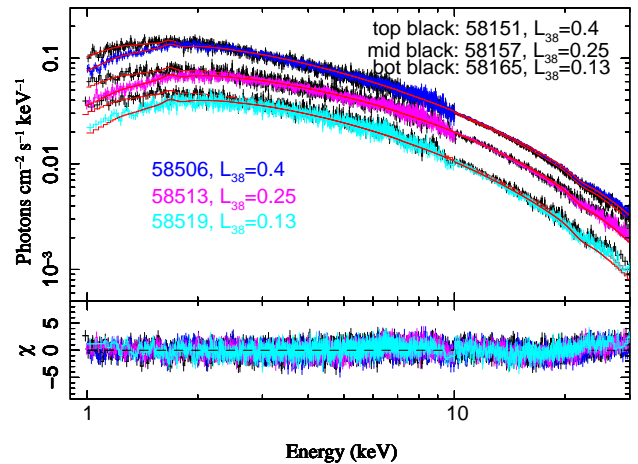


Figure 6. Comparison of the spectra extracted at similar luminosities from the giant outburst (MJD 58151, 58157, and 58165, black) and the last outburst (MJD 58506, 58513, and 58519, colored).

reported recently by Kong et al. (2022). It indicates that the dipole field of Swift J0243 is similar to the magnetic field measured near the neutron star.

The observed $\dot{\nu} - L$ relation around the transition regime of spin-up and spin-down shows an offset between the later period of the giant outburst (around MJD 58160) and the last outburst around MJD 58500. The zero point of $\dot{\nu} = 0$ is around $\sim 0.15 - 0.2 \times 10^{38}$ erg s $^{-1}$ for the giant outburst, while it is around $\sim 0.33 \times 10^{38}$ erg s $^{-1}$ for the last outburst. Such a phenomena is in contrast to the expectation of a simple torque model, which generally predicts a single $\dot{\nu} - L$ relation and a single point of zero torque. One possible reason is that for different outburst, the angular momentum of accreting material may have different normal direction, which may lead to a different accretion torque for similar accretion rate.

As pointed out by our anonymous referee, the two different zero-torques happen in different types of outbursts (the one around MJD 58160 is giant outburst, while the other one is from minor outbursts), which may have different accreting flows, and the difference of flows may be reflected in the spectrum and/or pulse profile. In Figure 6, we present the spectra from both the giant outburst and the last outburst at similar luminosities of $L_{38} \sim 0.13, 0.25,$ and 0.4 , with the fitting results listed in the bottom part of table 1. As can be seen, all three spectra of the giant outburst below 2 keV are systematically higher than those of the last outburst. The fitted absorption column densities of the giant outburst are typically less than those of the last outburst by $\sim 0.2 \times 10^{22}$ cm $^{-2}$. It indicates there is less material

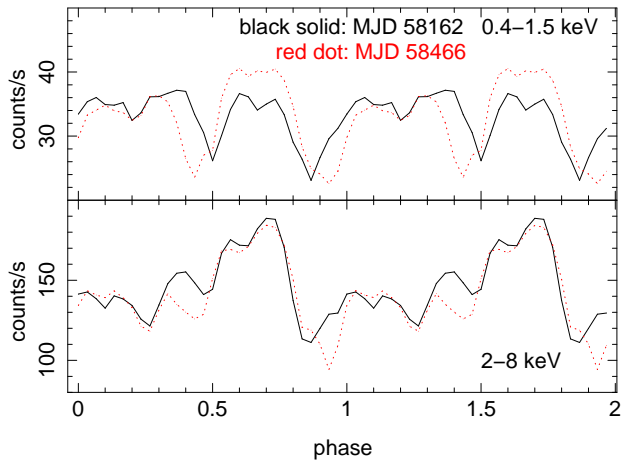


Figure 7. Comparison of the pulse profiles extracted from *Nicer* data at a similar luminosity of $L_{38} \sim 0.22$ from the giant outburst (black solid, MJD 58162) and the last outburst (red dot, MJD 58466) in 0.4-1.5 keV (top) and 2-8 keV (bottom).

between the emitting region of the neutron star and us for the giant outburst than for the last outburst.

The pulse profiles in 0.4-1.5 keV and 2-8 keV for two observations at a similar luminosity ($L_{38} \sim 0.22$) from the giant outburst (MJD 58162) and the last outburst (MJD 58466) are presented in Figure 7. These profiles are in the middle state between the spin-up and the low spin-down regime and are composed of three peaks. While the 2-8 keV profiles look quite similar, the 0.4-1.5 keV ones do show significant differences. The 0.4-1.5 keV main peak (around phase 0.7) of MJD 58162 is less significant than that of MJD 58466, while the two peaks around phase 0.2 of MJD 58162 are broader than that of MJD 58466. The differences of the spectra and low-energy pulse profiles at a similar luminosity between the giant outburst and the last outburst indicate that the accreting flows are likely different for different types of outburst, and the different flows can lead to different points of zero-torque.

The $\dot{\nu} - L$ relation during the spin-down regime shows a complex behavior. During the peak period of the minor outburst, the luminosity is relatively high and the $\dot{\nu}$ is relatively large, close to zero, as expected. On the other hand, during some lowest flux periods, the $\dot{\nu}$ is also close to zero, which is unexpected. This anomalous $\dot{\nu}$ behavior in the lowest spin-down regime may imply that there is much less material in this regime, or some other unknown reason. Further study is needed to reveal the real physical origin.

The pulse profile of Swift J0243 also shows significant evolution during the spin-up/spin-down transition.

The profile is double-peaked in the spin-up state, but it changes to a single broad peak around the luminosity of $L_{38} \sim 0.04 - 0.08$ during the spin-down regime. In-between, the profile shows a transitional shape. In order to provide a much broader peak in the low spin-down regime, the emission beam/region of the neutron star should be larger for the low spin-down regime than that for the spin-up regime. This may reflect the more stochastic nature of the accreting flow during the spin-down regime.

The spectral characteristic of Swift J0243 during the spin-down regime is continuous and gradual with decreasing luminosity, except at the lowest luminosity around $L_{38} \sim 0.05$. The changing trend is similar to those below an Eddington luminosity (Kong et al. 2020): both the photon index and cutoff energy decreases with decreasing luminosity. Such a behavior is similar to that of KS 1947+300 and EXO 2030+375, as reported by Reig & Nespoli (2013). It is interesting to note that the decreasing trend of photon index and cutoff energy of KS 1947+300 and EXO 2030+375 reversed below 0.2 and $1 \times 10^{37} \text{ergs}^{-1}$, respectively, and Swift J0243 shows a reversing trend around $0.5 \times 10^{37} \text{ergs}^{-1}$.

We note that the pulsation of Swift J0243 is still detected by *Nicer* observations even when the luminosity is much lower ($\sim 10^{35} \text{ergs}^{-1}$), as first illustrated by a *NuSTAR* observation on MJD 58557 (Doroshenko et al. 2020). The pulse profiles during these extremely low states are also a single broad peak. Nevertheless, the signal is too low to provide a reasonable estimation of $\dot{\nu}$. Based on the observed pulsation around 10^{34}ergs^{-1} , some previous work (e.g. Doroshenko et al. 2020; Kong et al. 2022) suggested that Swift J0243 has not reached a propeller state at such a low luminosity and inferred a weak dipole field. Nevertheless, the expectation of complete shutoff of accretion and pulsed emission during the propeller regime could be too ideal (e.g. Spruit & Taam 1993; Rappaport et al. 2004). For example, many accreting millisecond X-ray pulsars show pulsed emission when the accretion rate is expected in the propeller regime (e.g. Archibald et al. 2015; Papitto et al. 2015; Sanna et al. 2020). MHD simulations showed that accretion is still possible even when the magnetosphere radius is 5 times the co-rotation radius (e.g. Romanova et al. 2018). They proposed two reasons why accretion is possible when the magnetosphere rotates more rapidly than the inner disk: only the closed part of the magnetosphere rotates more rapidly than the inner disk and the process is non-stationary.

Our results show that the accretion process is still ongoing during the low spin-down regime of Swift J0243, when the accretion torque is much lower

than the braking torque. Many torque models predict a zero torque when the magnetosphere radius is close to the co-rotation radius (e.g. Wang et al. 1995; Kluźniak & Rappaport 2007). If this prediction is kind of true, the zero-torque luminosity ($L_{38} \sim 0.33$) implies that when the luminosity is 10 times smaller ($L_{38} \sim 0.03$), the magnetosphere radius would be about 2 times the co-rotation radius. That is, accretion is still ongoing when the magnetosphere radius is a little larger than the co-rotation radius (the propeller regime). The mechanism of accreting millisecond X-ray pulsar mentioned above may also apply to Swift J0243. The accretion geometry during this low spin-down regime is most likely changed, as evidenced by the change of the pulse profile.

Future more sensitive X-ray observatories will provide much great detail of the spin-down accretion regime of X-ray pulsars.

ACKNOWLEDGEMENTS

We thank our referee for helpful comments and suggestion of the effects of different accretion flows and Zhang Shuang-Nan for helpful discussions. This research is supported by National Natural Science Foundation of China (U1938113) and the Scholar Program of Beijing Academy of Science and Technology (DZ BS202002). This research used data obtained with *Nicer*, *Fermi/GBM*, *Swift*, and *HXMT*.

REFERENCES

- Archibald, A. M.; Bogdanov, S.; Patruno, A.; Hessels, J. W. T.; Deller, A. T.; Bassa, C.; Janssen, G. H.; Kaspi, V. M. et al. 2015, *ApJ*, 807, 62
- Bailer-Jones, C. A. L.; Rybizki, J.; Fouesneau, M.; Mantelet, G.; Andrae, R. 2018, *AJ*, 156, 58
- Bailer-Jones, C. A. L.; Rybizki, J.; Fouesneau, M.; Demleitner, M.; Andrae, R. 2021, *AJ*, 161, 147
- Basko, M. M. & Sunyaev, R. A. 1976, *MNRAS*, 175, 395
- Bildsten, L. et al. 1997, *ApJS*, 113 367
- Chakrabarty, D. et al. 1997, *ApJ*, 474, 414
- Doroshenko, V. et al. 2017, *MNRAS*, 466, 2143
- Frank, J., King, A., and Raine, D. 2002, *Accretion Power in Astrophysics*, Cambridge University Press
- Finger, M. H. et al. 2009, arXiv0912.3847
- Ghosh, P. & Lamb, F. K. 1979, *ApJ*, 234, 296
- Kluźniak, W. & Rappaport, S. 2007, *ApJ*, 671, 1990
- Kong, L. D.; Zhang, S.; Chen, Y. P. et al. 2020, *ApJ*, 902, 18
- Kong, L. D.; Zhang, S.; Zhang, S. N.; Ji, Long; Doroshenko, V.; Santangelo, A.; Chen, Y. P.; Lu, F. J. et al. 2022, *ApJ*, 933, L3
- Liu, J.; Jenke, P. A.; Ji, L.; Zhang, S.-N.; Zhang, S.; Ge, M.; Liao, J.; Li, X.; Song, L. 2022, *MNRAS*, 512, 5686
- Malacaria, C., Jenke, P., Roberts, O. J., Wilson-Hodge, C. A., Cleveland, W. H., Mailyan, B. 2020, *ApJ*, 896, 90
- Meegan, C. et al. 2009, *ApJ*, 702, 791
- Papitto, A.; de Martino, D.; Belloni, T. M.; Burgay, M.; Pellizzoni, A.; Possenti, A.; Torres, D. F. 2015, *MNRAS*, 449, L26
- Rappaport, S. & Joss, P. C. 1977, *Nature*, 266, 683
- Rappaport, S. A.; Fregeau, J. M.; Spruit, H. 2004, *ApJ*, 606, 436
- Reig, P. 2011, *Ap&SS*, 332, 1
- Reig, P. & Nespoli E. 2013, *A&A*, 551, 1
- Romanova, M. M.; Blinova, A. A.; Ustyugova, G. V.; Koldoba, A. V.; Lovelace, R. V. E. 2018, *NewA*, 62, 94
- Sanna, A.; Burderi, L.; Gendreau, K. C.; Di Salvo, T.; Ray, P. S.; Riggio, A.; Gambino, A. F.; Iaria, R.; Piga, L.; Malacaria, C., 2020, *MNRAS*, 495, 1641
- Spruit, H. C. & Taam, Ronald E. 1993, *ApJ*, 402, 593
- Tsygankov, S. S.; Doroshenko, V.; Mushtukov, A. A.; Lutovinov, A. A.; Poutanen, J. 2018, *MNRAS*, 479, L134
- Wang, Y. M. 1995, *ApJ*, 449, L153
- Wilson-Hodge, C. A.; Malacaria, C.; Jenke, P. A. et al. 2018, *ApJ*, 863, 9
- Zhang, S. N. et al. 2020, *SCPMA*, 63, 9502